Journal of Power Sources 204 (2012) 40–45

Contents lists available at SciVerse ScienceDirect

Journal of Power Sources

journal homepage: www.elsevier.com/locate/jpowsour

Performance enhancement of Ni-YSZ electrode by impregnation of $Mo_{0.1}Ce_{0.9}O_{2+\delta}$

Yu Chen [a], Jacob Bunch [a], Chao Jin [b], Chenghao Yang [a], Fanglin Chen [a,*]

[a] Department of Mechanical Engineering, University of South Carolina, 300 Main Street, Columbia, SC 29208, USA
[b] School of Energy, Soochow University, Suzhou 215006, Jiangsu, PR China

ARTICLE INFO

Article history:
Received 8 October 2011
Received in revised form
21 December 2011
Accepted 1 January 2012
Available online 9 January 2012

Keywords:
Solid oxide cells
Molybdenum-doped ceria
Ion-impregnation
Sulfur tolerance
Coking resistance

ABSTRACT

$Mo_{0.1}Ce_{0.9}O_{2+\delta}$ (MDC) impregnated nickel-yttria-stabilized zirconia (Ni-YSZ) has been fabricated and evaluated in both solid oxide fuel cell (SOFC) and solid oxide electrolysis cell (SOEC) modes. The optimal electrode performance has been obtained by MDC modified Ni-YSZ with MDC loading of about 294 mg cm^{-3} resulted from 7 repeated impregnation cycles. Single cells with the configuration of MDC modified Ni-YSZ as the hydrogen electrode, YSZ as the electrolyte and $(La_{0.75}Sr_{0.25})_{0.95}MnO_3$–YSZ as the oxygen electrode show a power density of 837 mW cm^{-2} and a polarization resistance of 0.15 Ω cm^2 (under open circuit condition) at 800 °C when using hydrogen as the fuel and ambient air as the oxidant in the SOFC mode. Such cells show current densities of 1.14 A cm^{-2} and 1.60 A cm^{-2} with 30 vol.% and 70 vol.% absolute humidity (AH), respectively at 800 °C with an applied voltage of 1.6 V in the SOEC mode. The cells with MDC modified Ni-YSZ as the anode also show very good sulfur tolerance and coking resistance. Power densities of 440 mW cm^{-2} and 420 mW cm^{-2} can be obtained when using H_2 with 50 ppm H_2S and methane as the fuel, respectively under a current density of 0.60 A cm^{-2} at 750 °C. It has been revealed that MDC enhances the electrical conductivity and improves the triple phase boundary (TPB) length, resulting in significant enhancement of the cell performance when using the MDC modified Ni-YSZ electrode.

1. Introduction

Solid oxide cells (SOCs) have been considered as one of the promising technologies, since they can be operated efficiently in the fuel cell mode by electrochemically combining fuel with oxidant (solid oxide fuel cell, SOFC) and the electrolysis mode by generating chemicals through electrolysis (solid oxide electrolysis cell, SOEC) [1,2]. SOFC has been reported to be reversible and can be operated in SOEC mode for fuel production. Therefore, the knowledge and experiences accumulated in the SOFC studies can be also beneficial to the SOEC research for achieving high and durable cell performance. For successful commercialization of the SOFC and SOEC technologies, however, the cost of the system must be reduced. One of the recognized cost reduction solutions is to reduce the operating temperature from the traditional 1000 °C to 600–800 °C, which allows the use of inexpensive metallic materials as interconnect and other components that reduce the manufacturing cost. In addition, the stability of the cell performance can also be significantly improved at the reduced cell operating temperature. However, operation at lower temperatures results in the overall electrochemical performance reduction due to the increased cell resistance, especially the cell polarization resistance (R_p).

The most commonly used hydrogen electrode for SOFCs and SOECs is nickel-yttria-stabilized zirconia (Ni-YSZ) cermet where Ni provides electronic conductivity as well as electrochemical activity for H_2 oxidation and H_2O reduction, while YSZ provides ionic conductivity and improves the adhesion between the Ni-YSZ electrode and the YSZ electrolyte. However, Ni-YSZ is susceptible to sulfur poisoning and carbon deposition when directly operating in sulfur-containing hydrocarbon fuels, resulting in severe deterioration of the cell performance. The mechanism of performance loss can be attributed to the physical adsorption/chemisorptions of H_2S or C at the active Ni surface sites [3,4]. To prevent sulfur poisoning and/or carbon deposition when using fuels with H_2S and/or hydrocarbon, certain strategies have been reported. For example, some electrolyte materials such as scandium stabilized zirconium and $BaZr_{0.1}Ce_{0.7}Y_{0.2-x}Yb_xO_{3-\delta}$ which promote oxidation of S or C due to their high ionic conductivity have replaced YSZ to improve the sulfur tolerance and carbon resistance of Ni-based cermet electrode [5,6]. Coating material such as ceria modification has also been explored on Ni surface [7]. It has been assumed that the presence of an ionic conducting phase with a large amount of O^{2-} may help remove sulfur and carbon in the form of SO_2 and CO_2 or CO [8,9].

The wet impregnation method has been proven to be an effective method to decrease the polarization resistance both in SOFC and SOEC modes [10]. Many groups have reported high electrocatalytic activity and enhanced stability of the electrode by

* Corresponding author. Tel.: +1 803 777 4875; fax: +1 803 777 0106.
E-mail address: chenfa@cec.sc.edu (F. Chen).

0378-7753/$ – see front matter © 2012 Elsevier B.V. All rights reserved.
doi:10.1016/j.jpowsour.2012.01.019

infiltrating the corresponding metal nitrate solution into the preformed porous YSZ backbone or the electrode substrates [11,12]. By impregnating the ionic or electronic conducting phase into the electrode, both the electrical conductivity and three phase boundary (TPB) length are greatly enhanced, and in turn, R_p is significantly decreased.

CeO_2-based oxide has been widely used in the automotive pollution control system due to its so-called oxygen storage capacity (OSC) ability, functioning as an oxygen buffer by storing/releasing O_2 due to the Ce^{4+}/Ce^{3+} redox couple, which forms an integral part of three-way catalysts for automotive exhaust treatment [13]. With higher OSC of the catalyst, higher conversion efficiency and resistance to thermal aging are generally observed [14]. It is reported that the OSC could be significantly enhanced by doping with titanium [15], zirconium [16] or molybdenum [17] due to the valence change of dopant or the structure distortion of the solid solution. MoO_3 has also shown catalytic activity in many application areas such as methanol oxidation [18] and toluene oxidation [19]. Recently, Mo-containing perovskites such as $Sr_2Mg_{1-x}Mn_xMoO_{6-\delta}$ [20] and $Sr_2Fe_{1.5}Mo_{0.5}O_6$ [21] have been developed as novel ceramic anode for SOFC applications, showing good tolerance to sulfur poisoning and anti-carbon deposition when operating the cell with hydrocarbon fuels. These perovskites exhibit high electronic conductivity in reducing environment due to the reduction of Mo^{6+}. MoO_3–CeO_2 catalysts have been employed as catalyst in the thermo-catalytic cracking (TCC) process [22] and CO oxidation [23]. The structure and electrical properties of Mo doped CeO_2 has been studied by Li et al. [24]. It is concluded that the 10 at.% Mo-doped CeO_2 exhibited electrical conductivities of 2.8×10^{-4} and 5.08×10^{-2} S cm^{-1} at 550 °C in air and wet H_2, respectively. Consequently, it is our hypothesis that by introducing ceria and Mo^{6+}/Mo^{5+} couple as a catalyst in the electrode, the cell performance, especially the sulfur tolerance and coking resistance, can be substantially enhanced.

In this study, NiO-YSZ/YSZ/$(La_{0.75}Sr_{0.25})_{0.95}MnO_3$ (LSM)–YSZ button cells with Ni-YSZ modified by 10 at.% MoO_3 doped CeO_2 ($Mo_{0.1}Ce_{0.9}O_{2+\delta}$, MDC) have been fabricated by an ion-impregnation method. The microstructure features, the impregnation loading effect on the cell performance, the electrochemical performance of the cells in both fuel cell and electrolysis modes as well as the long term stabilities of the cells in H_2 with 50 ppm H_2S and in methane have been systematically evaluated.

2. Experimental

2.1. Fabrication of the single cells

NiO-YSZ substrate was obtained by uniaxially pressing of a ball-milled mixture of NiO (Sigma–Aldrich, USA) and YSZ (8 mol% Y_2O_3, Tosoh Company, Japan) powders with 20 wt% graphite powder, and then pre-sintered at 800 °C for 2 h. Thin YSZ electrolyte layer was prepared by a similar dip-coating method. After co-sintering at 1400 °C for 5 h, a dense electrolyte layer was obtained. The $(La_{0.75}Sr_{0.25})_{0.95}MnO_3$ (LSM)–YSZ composite cathode with an effective area of ~0.33 cm^2 was prepared by screen-printing method and fired at 1100 °C for 2 h. The LSM powder was synthesized by the citric acid–nitrate method. A 0.5 M aqueous solution of $Ce(NO_3)_3{\cdot}6H_2O$ (Alfa Aesar, USA) and $(NH_4)_6Mo_7O_{24}$ (Alfa Aesar, USA) (atom ratio of Ce^{3+}:Mo^{6+} is 9:1) with citric acid (ratio of citric acid:cations is 3) was infiltrated into the NiO-YSZ substrate under vacuum. The anode was then dried at 60 °C for 12 h and sintered at 800 °C for 2 h. This cycle was repeated until a desirable MDC loading level was achieved. The MDC loading level was determined by the weight difference before and after each impregnation treatment cycle. We called cell without impregnation as Cell-0 and cells with 5, 7 and 9 impregnation times as Cell-5, Cell-7 and Cell-9, respectively.

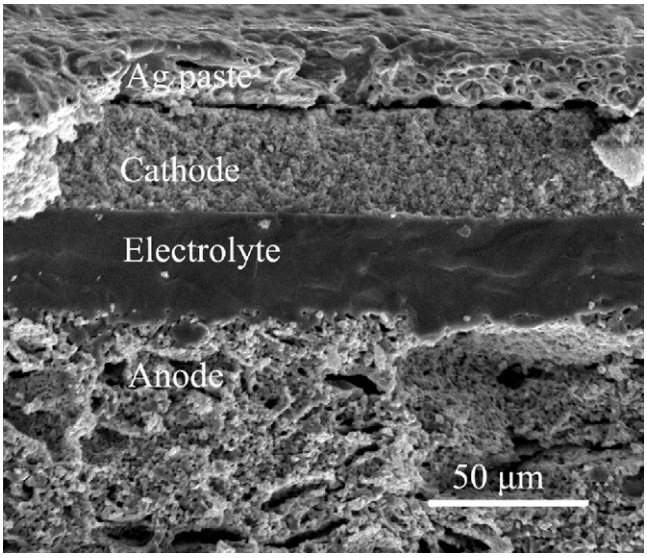

Fig. 1. Cross-section SEM image of the unmodified cell (Cell-0) after testing.

2.2. Cell testing

The current density–voltage curves as well as the impedance spectra were measured with a four probe method using a multi-channel Versa STAT (Princeton Applied Research) at the operating temperature range from 700 °C to 800 °C. The high temperature fuel cell and electrolysis testing system can be seen in our previous work [30]. During SOFC test, humidified hydrogen gas (3% H_2O/97% H_2) was used as fuel to the anode side while the cathode side was exposed to the ambient environment. During SOEC test, the amount of water vapor in the gas mixture was continuously measured in terms of absolute humidity (AH, the vol.% of humidity in the total gas volume) using an on-line humidity sensor (Vaisala Model HMP 337). Hydrogen flow rate was controlled at 45 sccm by a precision volume flow controller (APEX, Alicat Scientific). The cell polarization resistance (R_p) was determined from the difference between the low and high frequency intercepts of the impedance spectra with the real axis. The microstructure of the cell was characterized using a scanning electron microscope (SEM, FEI Quanta 200).

3. Results and discussion

3.1. Cell performance of cell without modification (Cell-0)

Fig. 1 shows the SEM image of the cross-section microstructure of the unmodified cell (Cell-0). The dense YSZ electrolyte about 30 μm thick is well adhered to both the anode and cathode. The thicknesses of the porous anode and cathode are about 0.85 mm and about 30 μm, respectively. There are some large flake-shaped pores in the anode, which are probably due to the flake-shaped graphite added as the pore former.

Fig. 2 shows the cell voltage, current and power output curves of Cell-0 at different temperature. The peak power density is 342, 434 and 531 mW cm^{-2} at 700, 750 and 800 °C, respectively. Fig. 3 shows the impedance spectra of Cell-0 measured at different temperatures under open-circuit conditions. The cell ohmic resistance (R_Ω), corresponding to the high-frequency intercept of the impedance spectra with the real axis, is 0.40, 0.28 and 0.21 Ω cm^2 at 700, 750 and 800 °C, respectively. The cell polarization resistance (R_p), determined from the difference between the high- and low-frequency

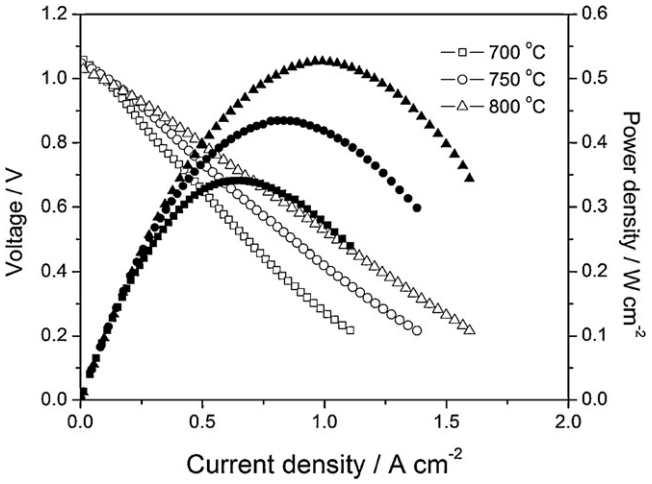

Fig. 2. IV and IP curves of the unmodified cell (Cell-0) at different temperatures when using H_2 as the fuel and air as the oxidant.

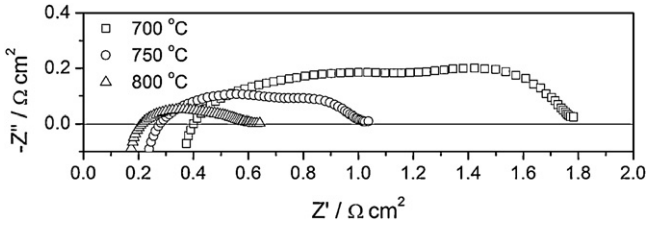

Fig. 3. Impedance spectra of the unmodified cell (Cell-0) tested at different temperatures under open circuit conditions.

intercepts of the impedance spectra with the real axis, is 1.39, 0.74 and 0.42 $\Omega\,cm^2$ at 700, 750 and 800 °C, respectively. The cell performance is comparable to the results reported by other groups for the similar cell configuration and testing conditions [25–27].

3.2. The effect of MDC impregnation

Table 1 is a summary of the effect of MDC impregnation in the anode on cell polarization resistance and cell peak power density. The results indicate that the cell performance is enhanced after impregnation. However, it can also be found that the cell performance enhancement from the MDC loading increases further until the seventh MDC infiltration cycle, and then decreases upon further increase in the repeated MDC infiltration. These results are in agreement with the previous reports for infiltrated electrode catalyst in SOFCs [28,29]. The optimum MDC loading is about 294 mg cm^{-3} after seven repeating infiltration cycles (Cell-7) in this study.

3.3. Fuel cell performance of Cell-7

Fig. 4 shows the cell voltage, current and power output curves of the cell with seven repeated MDC infiltration in the anode (Cell-7) at different temperatures when using hydrogen as the fuel and ambient air as the oxidant. The cell peak power density is as high as 581, 733 and 837 mW cm^{-2} at 700 °C, 750 °C and 800 °C, respectively. Fig. 5 shows the impedance spectra of Cell-7 measured at different temperatures under open circuit conditions. Both the cell ohmic resistance (R_Ω) and polarization resistance (R_p) decreased after impregnation of MDC in the anode, indicating that the attachment between the anode and electrolyte, microstructure of the anode as well as the catalytic activity of the anode have been greatly optimized through MDC infiltration.

Table 1
The R_p and peak power density of cell after different infiltration cycles tested at 700 °C, 750 °C and 800 °C, respectively.

Cell	R_p ($\Omega\,cm^2$)			Peak power density (mW cm^{-2})		
	700 °C	750 °C	800 °C	700 °C	750 °C	800 °C
Cell-0	1.39	0.74	0.42	342	434	531
Cell-5	0.59	0.33	0.21	415	542	765
Cell-7	0.30	0.24	0.15	581	733	837
Cell-9	0.59	0.29	0.20	411	535	763

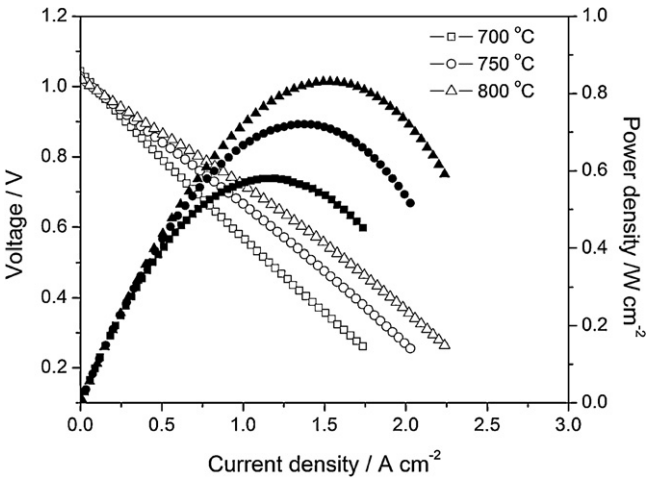

Fig. 4. IV and IP curves of Cell-7 tested at different temperatures using hydrogen as the fuel and air as the oxidant.

3.4. Electrolysis cell performance of Cell-7

Fig. 6(a) and (b) shows the polarization performances of Cell-7 under the SOEC mode. H_2 flow rate was set at 45 sccm and the absolute humidity (AH) was varied from 30 vol.% to 70 vol.% in the hydrogen electrode gas stream while the oxygen electrode was exposed to ambient air. The data were acquired by decreasing the potential from 1.8 to 0.2 V with a 30 mV s^{-1} voltage sweeping rate, as displayed in Fig. 6(a). The applied cell voltages are plotted as a function of the cell current densities. Negative current densities indicate electrolysis mode, and the cell voltage at zero current density corresponds to the OCV. As shown in Fig. 6(a), OCV is influenced by the steam to hydrogen ratio, and increases when the steam to hydrogen ratio decreases, as predicted from the Nernst equation for the hydrogen–oxygen–steam system, which can be seen in our previous work [30]. In the SOEC mode, the voltage varies linearly with the cell current density. It can be seen that the increase either in the cell operating temperature or AH in the hydrogen electrode gas stream can lead to the improvement of the cell current density values. For example, according to Fig. 6(b), at 70 vol.% AH, a cell current density value of 0.68 A cm^{-2} was observed at 700 °C, while it increased to 1.65 A cm^{-2} at 800 °C with an applied cell voltage of 1.6 V; on the other hand, at 800 °C, when the AH was increased from 30 to 70 vol.%, the cell current density showed a significant improvement, from 1.14 to 1.65 A cm^{-2}, comparable to our previous study with the modified oxygen electrode of the SOECs [31]. In

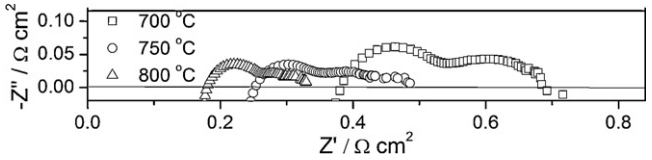

Fig. 5. Impedance spectra of Cell-7 measured at different temperatures under open circuit conditions.

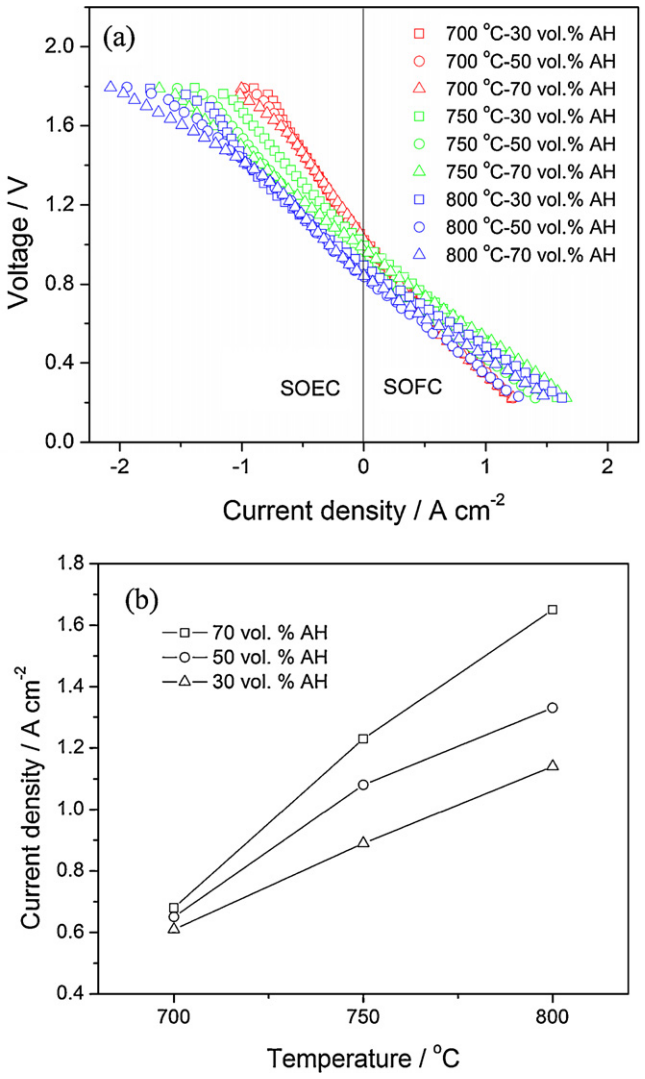

Fig. 6. (a) Voltage–current density of Cell-7 and (b) current density under an applied voltage of 1.6 V recorded as a function of different operating temperatures and absolute humidity.

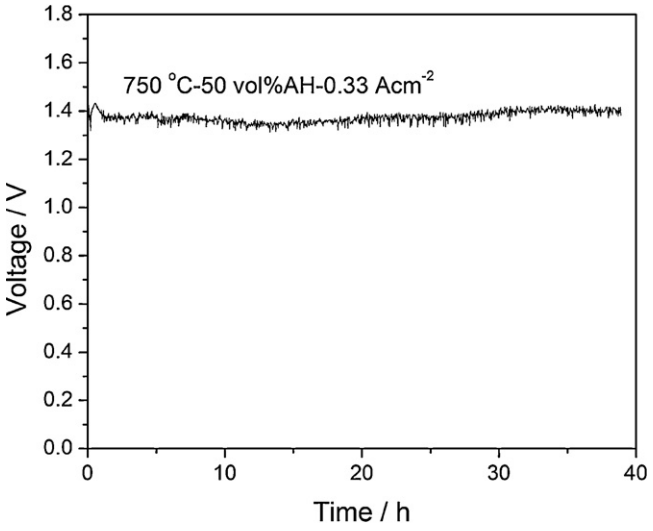

Fig. 7. Short term electrolysis testing of Cell-7 with an applied current of 0.33 A cm^{-2} operated at 750 °C and 50 vol.% absolute humidity.

this work, LSM–YSZ oxygen electrode was fabricated by mechanically mixing of LSM and YSZ powders instead of the infiltration method to enhance the oxygen electrode performance. Therefore, it can be concluded that the enhancement of the cell performance in this study can be attributed to MDC modification on the Ni-YSZ.

Fig. 7 shows the short term stability of Cell-7 under electrolysis operation at 750 °C and 50 vol.% AH. The cell was operated at a constant current density of 0.33 A cm^{-2}, and the cell voltage was recorded to evaluate the cell performance stability. The cell voltage required to maintain a 0.33 A cm^{-2} electrolysis current density is plotted as a function of the operating time. Overall the cell shows a very stable performance in the period tested.

Fig. 8 shows the SEM images of the hydrogen electrode of Cell-7 before and after the short-term electrolysis testing. It can be seen that the surfaces of Ni and YSZ particles were fully covered by the nano-sized MDC particles. The connection between the YSZ electrolyte and the Ni-YSZ hydrogen electrode was enhanced by impregnation of MDC since the pores in this area were partially filled with MDC. Consequently, the MDC impregnation significantly enhanced the hydrogen electrode performance by increasing the TPB length and the electrical conductivity. Further, there is no observable microstructure change in the MDC infiltrated hydrogen electrode before and after the short-term electrolysis testing, indicating that the MDC infiltrated hydrogen electrode has good stability under the cell operating conditions.

3.5. Sulfur tolerance and carbon resistance

Fig. 9 shows the sulfur tolerance test of the MDC modified Ni-YSZ anode at 750 °C in the SOFC mode under a current density of 0.6 A cm^{-2}. The cell performance using H_2 as the fuel increased and then stabilized after operating for 100 h. The initial increase in cell performance was probably attributed to NiO reduction to Ni in the anode and the activation of the LSM–YSZ cathode. Upon stabilization of the cell performance, the fuel was switched from H_2 to H_2 containing 50 ppm H_2S. The process seems to have four stages: a rapid increase (1.35%) in the cell performance at first several minutes followed by a short-term stabilization for about 3 h and then a slow but continuous performance increase (1.33%) in the next 3 h, and at last a continuous drop (2.62%) in the following 32 h. Upon removal of H_2S from the fuel, the cell performance initially decreased but then gradually stabilized. After switching from H_2 to H_2 with H_2S, the cell performance increased first and then decreased again. Liu et al. pointed out that ceria can strongly absorb S and may be effective for electrochemical removal of S [32]. However, it needs to be pointed out that there is an initial increase, instead of a drop, in cell power output upon exposure to H_2 containing 50 ppm H_2S. In addition, it has been shown that the cell performance in H_2 with 50 ppm H_2S is higher than that in H_2, which is totally different from other coating materials such as ceria modified anode [7]. This may be attributed to the formation of MoS_2 from decomposition of H_2S, consequently leading to an increase in the dissociated hydrogen species [33]. Further, the formation of surface oxides such as MoS_2 [34] and Ni–Mo–S [35] can extend electrochemically active sites and improve the electrical conductivity [36].

Fig. 10 shows the short term stability test when using CH_4 as the fuel at 750 °C under a current density of 0.60 A cm^{-2}. The cell performance increased and then stabilized after operating for 40 h. Upon switching the fuel from H_2 to CH_4, the cell voltage output dropped from 705 mV to 483 mV in the first several minutes. The cell performance subsequently increased continuously in the next 50 h. Cell voltage eventually stabilized at about 698 mV and showed very stable cell performance in CH_4 for 200 h. The cell performance stability of the MDC-modified Ni-YSZ anode operating in methane as the fuel is much better than that of cells with Ni-based cermet

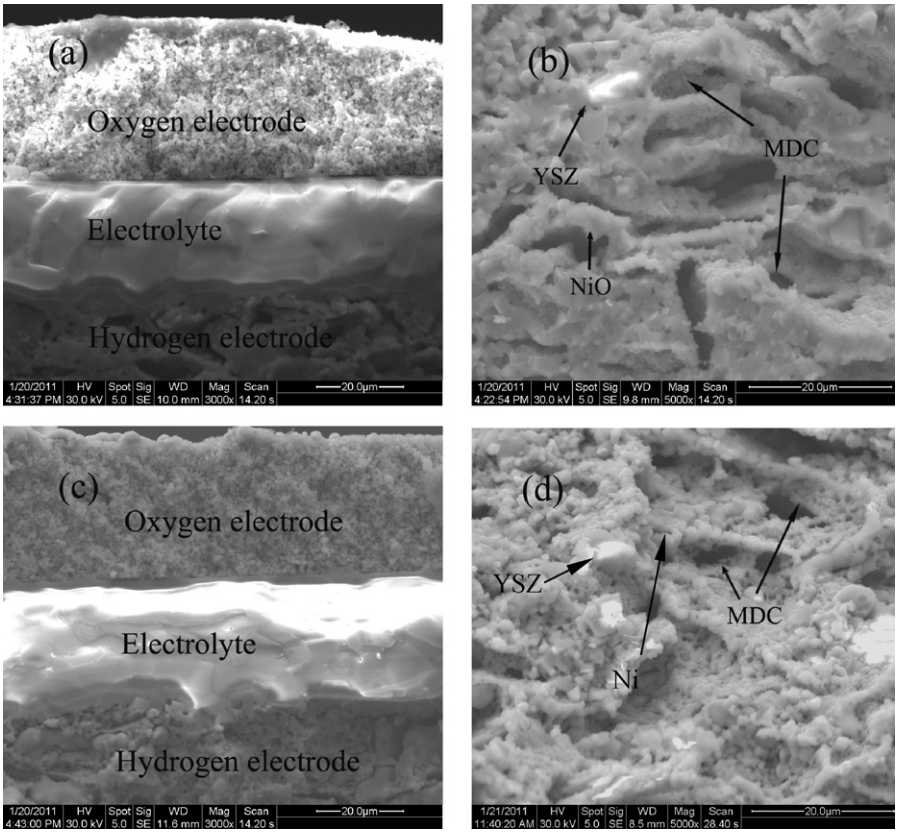

Fig. 8. SEM images of Cell-7 before and after short-term electrolysis testing: (a) cross-section view of the cell before testing; (b) microstructure of the hydrogen electrode before testing; (c) cross-section view of the cell after testing; (d) microstructure of the hydrogen electrode after testing.

modified by other ceria coating such as samaria-doped ceria (SDC) [28]. The enhancement of the cell performance stability operating in methane as the fuel may be attributed to the incorporation of molybdenum in ceria, resulting in a significant improvement to coking resistance [37] while having no adverse effect on the reforming activity [38]. It has been revealed that the coated MDC on Ni-YSZ anode not only effectively prevents the methane fuel from directly impacting on the Ni particles, but also enhances the kinetics of methane oxidation due to an improved oxygen storage capacity

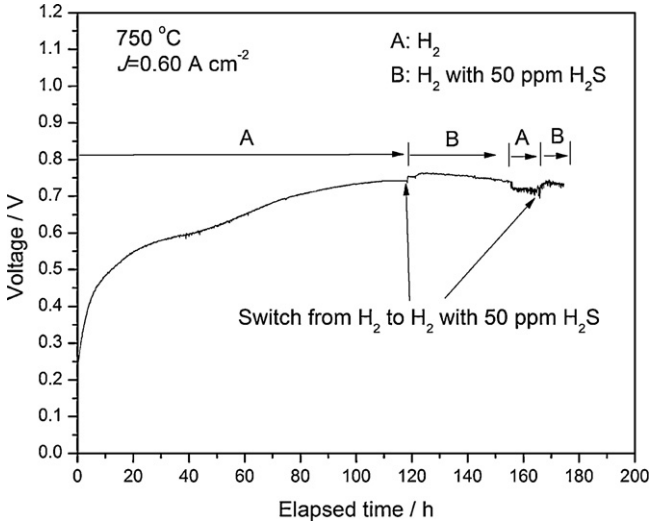

Fig. 9. Sulfur tolerance test for Cell-7 under a current density of 0.60 A cm^{-2} at 750 °C using H_2 and H_2 with 50 ppm H_2S as the fuel, respectively.

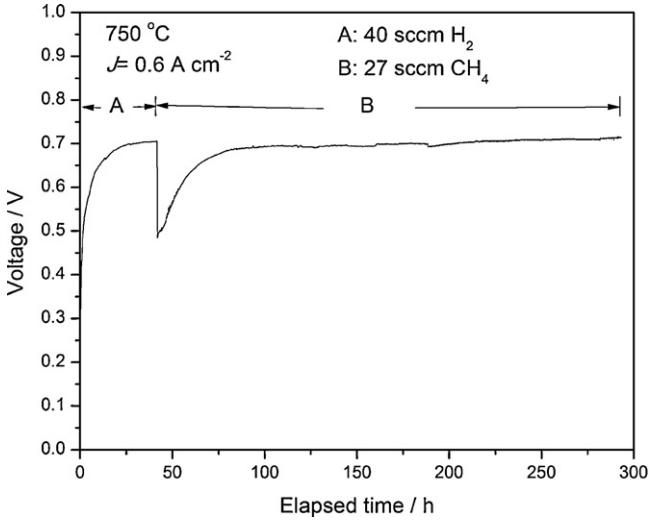

Fig. 10. The short-term cell performance testing of Cell-7 under a current density of 0.6 A cm^{-2} at 750 °C using H_2 and methane as the fuel, respectively.

(OSC) and redox equilibrium of the anode surface, resulting in significant enhancement of the MDC modified Ni-YSZ anode for direct methane oxidation.

4. Conclusions

The conventional Ni-YSZ electrode with 10 at.% Mo-doped CeO_2 (MDC) modification by an impregnation method has been evaluated for solid oxide fuel and electrolysis cells. The loading level of MDC has shown substantial impact on the electrochemical

performance of the resulted electrode. The electrode modified with MDC with a loading of about 294 mg cm^{-3} after 7 impregnation cycles shows the most improved performance. In the SOFC mode, the optimal cell shows a peak power density of 837 mW cm^{-2} and a polarization resistance of 0.15 Ω cm^2 (under open circuit condition) at 800 °C when using H_2 as the fuel. In the SOEC mode, current densities of 1.14 A cm^{-2} and 1.60 A cm^{-2} can be obtained at 30 vol.% and 70 vol.% absolute humidity (AH) at 800 °C with an applied voltage of 1.6 V, respectively. The anode modified by MDC also showed a very good sulfur tolerance using H_2 containing 50 ppm H_2S and coking resistance. The results indicated that the nano-sized MDC can greatly enhance the hydrogen electrode performance in both SOFCs and SOECs.

Acknowledgement

Financial support from the National Science Foundation (award no. 0967166) is greatly appreciated.

References

[1] A. Hauch, S.H. Jensen, S. Ramousse, M. Mogensen, J. Electrochem. Soc. 153 (2006) A1741–A1747.
[2] J.E. O'Brien, C.M. Stoots, J.S. Herring, P.A. Lessing, J.J. Hartvigsen, S. Elangovan, J. Fuel Cell Sci. Technol. 2 (2005) 156–163.
[3] M. Gong, X. Liu, J. Trembly, C. Johnson, J. Power Sources 168 (2007) 289–298.
[4] H. He, J.M. Hill, Appl. Catal. A: Gen. 317 (2007) 284–292.
[5] K. Sasaki, K. Susuki, A. Iyoshi, M. Uchimura, N. Imamura, H. Kusaba, Y. Teraoka, H. Fuchino, K. Tsujimoto, Y. Uchida, N. Jingo, J. Electrochem. Soc. 153 (2006) A2023–A2029.
[6] L. Yang, S. Wang, K. Blinn, M. Liu, Z. Liu, Z. Cheng, M. Liu, Science 326 (2009) 126–129.
[7] H. Kurokawa, T.Z. Sholklapper, C.P. Jacobson, L.C.D. Jonghe, S.J. Visco, Electrochem. Solid-State Lett. 10 (2007) B135–B138.
[8] I.V. Yentekakis, C.G. Vayenas, J. Electrochem. Soc. 136 (1989) 996–1002.
[9] E.P. Murray, T. Tsai, S.A. Barnett, Nature 400 (1999) 649–651.
[10] S.P. Jiang, Mater. Sci. Eng. A 418 (2006) 199–210.
[11] R. Craciun, S. Park, R.J. Gorte, J.M. Vohs, C. Wang, W.L. Worrell, J. Electrochem. Soc. 146 (1999) 4019–4022.
[12] C. Yang, C. Jin, F. Chen, Electrochem. Commun. 12 (2010) 657–660.
[13] A. Trovarelli, Catal. Rev.: Sci. Eng. 38 (1996) 439–520.
[14] J. Kaspar, P. Fornasiero, M. Graziani, Catal. Today 50 (1999) 285–298.
[15] G. Dutta, U.V. Waghmare, T. Baidya, M.S. Hegde, K.R. Priolkar, P.R. Sarode, Chem. Mater. 18 (2006) 3249–3256.
[16] S. Pengpanich, V. Meeyoo, T. Rirksomboon, Catal. Today 93–95 (2004) 95–105.
[17] D. Tibiletti, E.A.B. de Graaf, S. Pheng Teh, G. Rothenberg, D. Farrusseng, C. Mirodatos, J. Catal. 225 (2004) 489–497.
[18] C. Louis, J.M. Tatibouët, M. Che, J. Catal. 109 (1988) 354–366.
[19] M.W. Xue, X.D. Gu, J.P. Chen, H.L. Zhang, J.Y. Shen, Thermochim. Acta 434 (2005) 50–54.
[20] Y.H. Huang, R.I. Dass, Z.L. Xing, J.B. Goodenough, Science 312 (2006) 254–257.
[21] Q. Liu, X. Dong, G. Xiao, F. Zhao, F. Chen, Adv. Mater. 35 (2010) 10039–10044.
[22] N. Al-Yassir, R. Le Van Mao, Appl. Catal. A: Gen. 332 (2007) 273–288.
[23] M.M. Mohamed, S.M.A. Katib, Appl. Catal. A: Gen. 287 (2005) 236–243.
[24] Q. Li, V. Thangadurai, Fuel Cells 9 (2009) 684–698.
[25] L. Zhang, J. Gao, M. Liu, C. Xia, J. Alloys Compd. 482 (2009) 168–172.
[26] L. Zhang, S.P. Jiang, W. Wang, Y. Zhang, J. Power Sources 170 (2007) 55–60.
[27] C. Wang, W.L. Worrell, S. Park, J.M. Vohs, R.J. Gorte, J. Electrochem. Soc. 148 (2001) A864–A868.
[28] W. Zhu, C. Xia, J. Fan, R. Peng, G. Meng, J. Power Sources 160 (2006) 897–902.
[29] D. Ding, W. Zhu, J. Gao, C. Xia, J. Power Sources 179 (2008) 177–185.
[30] C. Yang, A. Coffin, F. Chen, Int. J. Hydrogen Energy 35 (2010) 3221–3226.
[31] C. Yang, C. Jin, A. Coffin, F. Chen, Int. J. Hydrogen Energy 35 (2010) 5187–5193.
[32] M. Liu, Z. Cheng, Y. Choi, J. Wang, S. Zha, Presented at DOE Sixth Annual SECA Workshop, Sulfur-tolerant Anode for SOFCs, Monterey, CA, April, 2005.
[33] S.H. Choi, Degree thesis, Georgia Institute of Technology, December 2007.
[34] T. Chivers, J.B. Hyne, C. Lau, Int. J. Hydrogen Energy 5 (1980) 499–506.
[35] W. Niemann, B. Clausen, H. Topsøe, Catal. Lett. 4 (1990) 355–363.
[36] A. Aoshima, H. Wise, J. Catal. 34 (1974) 145–151.
[37] L. Kepinski, B. Stasinska, T. Borowiecki, Carbon 38 (2000) 1845–1856.
[38] C.M. Finnerty, N.J. Coe, R.H. Cunningham, R.M. Ormerod, Catal. Today 46 (1998) 137–145.